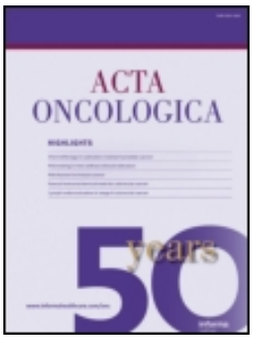

Acta Oncologica

ISSN: 0284-186X (Print) 1651-226X (Online) Journal homepage: informahealthcare.com/journals/ionc20

Are IMRT treatments in the head and neck region increasing the risk of secondary cancers?

Oscar Ardenfors, Dan Josefsson & Alexandru Dasu

To cite this article: Oscar Ardenfors, Dan Josefsson & Alexandru Dasu (2014) Are IMRT treatments in the head and neck region increasing the risk of secondary cancers?, Acta Oncologica, 53:8, 1041-1047, DOI: 10.3109/0284186X.2014.925581

To link to this article: https://doi.org/10.3109/0284186X.2014.925581

Acta Oncologica, 2014; 53: 1041–1047

informa
healthcare

ORIGINAL ARTICLE

Are IMRT treatments in the head and neck region increasing the risk of secondary cancers?

OSCAR ARDENFORS[1,2,3], DAN JOSEFSSON[2] & ALEXANDRU DASU[2]

[1]*Medical Radiation Physics, Department of Physics, Stockholm University, Stockholm, Sweden,*
[2]*Department of Radiation Physics and Department of Medical and Health Sciences, Linköping University, Linköping, Sweden and* [3]*Department of Medical Physics, Karolinska University Hospital, Stockholm, Sweden*

ABSTRACT

Background. Intensity-modulated radiation therapy (IMRT) has been increasingly employed for treating head and neck (H&N) tumours due to its ability to produce isodoses suitable for the complex anatomy of the region. The aim of this study was to assess possible differences between IMRT and conformal radiation therapy (CRT) with regard to risk of radiation-induced secondary malignancies for H&N tumours.

Material and methods. IMRT and CRT plans were made for 10 H&N adult patients and the resulting treatment planning data were used to calculate the risk of radiation-induced malignancies in four different tissues. Three risk models with biologically relevant parameters were used for calculations. The influence of scatter radiation and repeated imaging sessions has also been investigated.

Results. The results showed that the total lifetime risks of developing radiation-induced secondary malignancies from the two treatment techniques, CRT and IMRT, were comparable and in the interval 0.9–2.5%. The risk contributions from the primary beam and scatter radiation were comparable, whereas the contribution from repeated diagnostic imaging was considerably smaller.

Conclusion. The results indicated that the redistribution of the dose characteristic to IMRT leads to a redistribution of the risks in individual tissues. However, the total levels of risk were similar between the two irradiation techniques considered.

The use of intensity-modulated radiation therapy (IMRT) for head and neck (H&N) tumours has greatly increased in recent years as it has the potential to deliver complex dose distributions suitable for avoiding critical structures close to the target. However, concerns were raised from the point of view of the associated risks for second cancer from IMRT in comparison to three-dimensional (3D) conformal radiation therapy (CRT) [1–3]. Indeed, IMRT uses more treatment fields to modulate the fluence and this leads to a larger spread of the entrance dose and to a reduction of the volume of highly irradiated tissue. Furthermore, IMRT also requires an increased number of monitor units (MU) and therefore longer irradiation times, raising concerns about the increase in dose from head leakage and collimator scatter [3].

Epidemiological studies have shown that conventional radiation therapy is associated with a small but significant risk for radiation-induced second malignancies [4–7]. Results are not yet available for current techniques like IMRT due to the long latency of carcinogenesis. However, the impact of several of the aspects under consideration for IMRT has been explored in theoretical studies and their results illustrate the complexity of the risk problem for advanced treatment methods [1,8–12]. Nevertheless, other aspects characteristic to modern treatment methods, like the use of image guidance during treatment should be considered in the analysis of the risk. The analysis would have to simultaneously account for as many dose contributors as possible, as the dose response curve for risk is most likely non-linear at high doses [2,13].

Therefore, the aim of this study was to investigate the potential differences in the risk of radiation-induced second malignancies from IMRT in

Correspondence: O. Ardenfors, Medical Radiation Physics, Department of Physics, Stockholm University, Box 260, 17176 Stockholm, Sweden. Tel: +46 70 3458030. E-mail: oscar.ardenfors@ki.se

(Received 24 March 2014; accepted 13 May 2014)

ISSN 0284-186X print/ISSN 1651-226X online © 2014 Informa Healthcare
DOI: 10.3109/0284186X.2014.925581

comparison with CRT for the treatment of H&N tumours, including the effects of dose redistribution, the impact of scatter radiation and frequent imaging for target verification during the treatment. The robustness of the findings was also explored by employing three theoretical risk models with different dose-risk relationships.

Material and methods

Patient data and treatment planning

Risk assessments were carried out for 10 adult patients with H&N tumours located in either the base of the tongue, the hypopharynx or the tonsils. For each patient two plans were created, an IMRT plan using a sliding-window technique with 6 MV photons and a clinically equivalent CRT plan according to the routine clinical practice at the time of their treatment. The treatment plans were calculated with the Analytical Anisotropic Algorithm (AAA) on an Eclipse treatment planning system (Varian, Palo Alto, CA, USA). The prescribed dose to the tumour was 68 Gy delivered in 2 Gy daily fractions. A margin of 3–5 mm between the clinical target volume (CTV) and the planning target volume (PTV) was applied in accordance with standard protocol at the home institution. Dose-volume histograms (DVH) from all 20 treatment plans (10 patients with both an IMRT and a CRT treatment plan) were used for risk estimations. IMRT treatments employed more fields for all patients and consequently an overall increase in MUs with an average of 875 MUs for IMRT in comparison to 250 MUs for CRT (Supplementary Table I, available online at http://informahealthcare.com/doi/abs/10.3109/0284186X.2014.925581).

Four tissues of interest were included in the calculations: parotid glands, oesophagus, lungs and the remaining tissues (denoted "body" henceforth). The body was defined as all non-delineated tissues included in the CT data for each patient, i.e. PTV and the organs at risk (OAR) were excluded. The tissues were chosen based on their high radiosensitivity [14], large volumes, or location relative to the primary treatment beam.

Dose contribution and risk assessment

Risk calculations were performed on all 20 treatment plans taking three dose contributors into account: primary treatment radiation, secondary radiation from treatment head scatter and internal scatter, and imaging radiation from repeated cone-beam computed tomography (CBCT) sessions.

The radiation burden to the parotid glands, oesophagus and the body from the primary treatment beam was quantified through DVH calculations using the acquired treatment planning data from the corresponding IMRT and CRT treatment plans.

The dose contribution to the lungs from secondary scattered radiation was estimated through measurements using thermo-luminescence-dosimeters (TLDs) placed in an anthropomorphic phantom (CIRS ATOM adult female phantom model #702-004). The detectors were placed in two or four different regions in four different planes of the lungs, where the distance of the detectors relative to the caudal border of the PTV ranged from approximately −1 cm to +15 cm (Table I). The phantom was irradiated with a standard IMRT treatment plan and subsequently (after read-out) with a standard CRT treatment plan. This allowed the derivation of representative doses per MU for each treatment technique which were then used to calculate an estimate of the total contribution from secondary scattered dose to the lungs for all patients, for all number of fractions (34) and the average number of MUs per fraction. As this measurement methodology does not discriminate between head scatter and internal patient scatter, the result corresponds to total dose contribution to the lungs from scattered radiation.

The CBCT-associated dose burden for setup verification was calculated using results of a study [15] reporting doses relevant for the same system in use at the home institution at the time of the study, a Varian OBI 1.4 system. Thus, the estimated doses per CBCT scan were 1.5 mGy to the oesophagus, 4.8 mGy to the body, 5.1 mGy and 6.3 mGy to the left and right parotid gland, respectively. The CBCT imaging was assumed to be performed once every week during the radiation therapy treatment, but the influence of more frequent imaging on the total risk was also investigated as it is believed that it will have a relevant impact on the dose for other treatment sites [16].

The dose contribution from CBCT imaging was added to the treatment DVHs to account for the total radiation burden of the tissues of interest before

Table I. Doses from TLD measurements in an anthropomorphic phantom. Doses per MU are presented per fraction, average total doses and the corresponding ratios correspond to doses per MU per fraction multiplied with 34 fractions and the mean number of MUs employed for each treatment technique.

Distance from PTV (cm)		Dose per MU (mGy)		Av. Tot. Dose (Gy)		Av. Tot. Dose Ratio (IMRT/CRT)
IMRT	CRT	IMRT	CRT	IMRT	CRT	
−1.2	−0.7	1.72	7.61	51.2	64.6	0.8
4.1	4.6	0.05	0.19	1.5	1.6	1.0
9.2	9.7	0.03	0.08	0.8	0.6	1.2
14.5	15.0	0.02	0.05	0.6	0.4	1.6

the calculation of the risk. The lungs were not fully included in the patient CT planning data or in the CBCT field. Therefore the DVH data from the treatment planning system and the dose contribution from the CBCT were not included in the calculation of the risk to the lungs. Thus, the risk to the parotid glands, oesophagus and body from the primary beam and CBCT imaging was estimated using DVHs, and the risk to the lungs was estimated through calculations using the dose distribution in the lungs obtained through TLD-measurements at different distances from the PTV specified in Table I.

Risk models and parameters

Two bell-shaped models and one plateau-shaped model were used for calculations. The competition model predicts a bell-shaped dependence and is based on the assumption of a competition between the induction of carcinogenic mutations and cell kill taking into account fractionation effects [2]. The linear-exponential (lin-exp) model is similar to the competition model, but neglects fractionation effects [17]. The plateau model describes the induction of mutations in a population of precancerous cells leading to a saturation of the risk for higher doses as a result of the balance between malignant cell creation and mutated cell kill [18]. It should be noted that Schneider [19] showed that the plateau model could also lead to a bell-shaped dependence if the number of precancerous cells is affected by cell kill. The details of the models are given in the supplementary material of this article.

The risk to the lungs from secondary scattered dose was estimated using the average doses to each plane of the lungs presented in Table I. The risk was calculated for each plane of the lungs separately using the three risk models and then weighted for each corresponding risk model. The risk to the parotid glands, oesophagus and the body from heterogeneous irradiations has been calculated as the weighted average of the partial risks throughout the volume (Equation 1) as proposed by Dasu et al. [2].

$$Total\ risk = \frac{\sum Risk(D_i) \times V_i}{\sum V_i} \quad (1)$$

where $Risk(D_i)$ is the calculated risk for a volume of the irradiated tissue V_i receiving dose D_i.

The parameters for the risk models used in the study were derived from radiation protection recommendations and from epidemiological data as detailed in the supplementary material. Variations in organ sizes between individuals were accounted for by the use of a volumetric factor which assumes that the risk of radiation-induced cancer is related to the number of mutated cells which in turn is proportional to the volume of the irradiated tissue. This assumption takes into account interpatient variations in the size of the tissue cell populations irradiated [20,21] and is the same principle as behind Equation 1, namely that a larger tissue volume irradiated to a dose linked to a certain risk has a larger weight towards the total risk.

All non-radiation associated risk factors were excluded in this study, and the term "risk" will henceforth refer to the total lifetime radiation attributable risk of secondary cancer induction.

Results

Risk from primary treatment radiation

IMRT was found to expose larger volumes of the body to intermediate dose levels where the plateau model predicted high risks whereas in the same dose interval the bell-shaped models predicted a smaller risk as illustrated by Figure 1. This was, however, only one part of the comparison of the risk from IMRT and CRT and the average total risk of developing secondary malignancies in the body from IMRT was comparable to the corresponding risk from CRT according to all risk models as shown by the results in Figure 2. The corresponding risk in the oesophagus was higher for CRT according to the bell-shaped models, but comparable according to the plateau model. This difference originated from the average increase in absorbed dose to oesophagus (17.8 Gy for IMRT vs. 12.0 Gy for CRT) and its impact on the bell-shaped and the plateau risk models. Seven patients showed an identical relationship between IMRT and CRT with the one illustrated in Figure 2, while three showed a small increase for CRT over IMRT with the plateau model. The average differences between IMRT and CRT in risk to individual tissues for all patients were: 0.02%, 0.10% and 0.02% for the competition model; 0.03%, 0.01%, and 0.00% for the plateau model; 0.02%, 0.11% and 0.02% for the lin-exp model, for the body, oesophagus and parotid glands, respectively. The spread in risk to different tissues between patients indicated that the redistribution of dose (and consequently the risk) to the OARs associated with IMRT and CRT tends to cancel out giving similar results of the total risk for each risk model. No correlation between differences in calculated risks and different primary tumour sites could be seen, but the size of the investigated population was quite small to allow a more detailed analysis.

Risk from head- and internal scatter radiation

The doses per MU to the different lung planes in the anthropomorphic phantom are presented in Table I together with the average total dose contribution

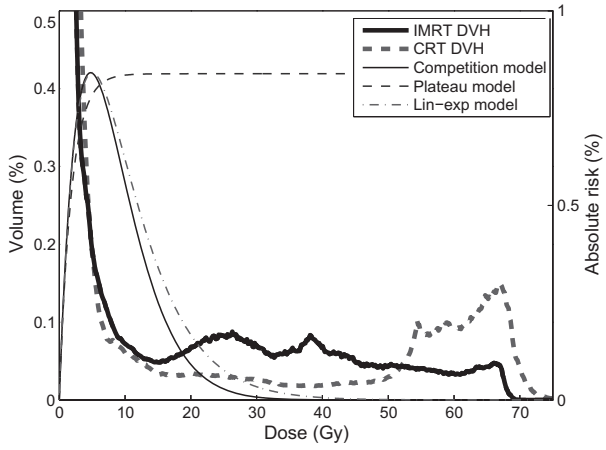

Figure 1. Differential DVH of the body for a typical H&N patient calculated for IMRT and CRT together with the dose dependence of the risk models included in the study.

(multiplied with 34 fractions and the average number of MUs per fraction for each technique). The TLD measurements showed that CRT delivered on average 3.3 times more in dose per MU compared to IMRT, consequently cancelling out the corresponding increase in average MUs employed in IMRT. It can also be seen that the relative dose contribution from IMRT was smaller inside the PTV and increased with increasing distance to the target.

Risk from CBCT imaging

The doses from the weekly CBCT examinations were relatively small causing little effect on the DVHs in comparison to the treatment-associated radiation burden. This led to the predicted total risk accounting for the imaging dose being only slightly higher than the risk neglecting this contribution for all risk models (Table II). Furthermore, even when assuming daily CBCT imaging the risk contribution was still considerably smaller than the risk from the primary treatment beam. Thus, the influence of positioning imaging on the total risk was deemed almost negligible in comparison to the treatment-associated risk.

Total risk from treatment, scatter and CBCT imaging

The predicted average total risk from IMRT or CRT treatment, scattered radiation to the lungs and weekly CBCT imaging was in the interval of 0.9–2.5% depending on the risk model, as shown by the results in Table II. The differences in total risk between treatment techniques were small according to all risk models indicating that no significant change in incidence of radiation-induced tumours should be expected for H&N patients treated with 6 MV photons using CRT or IMRT.

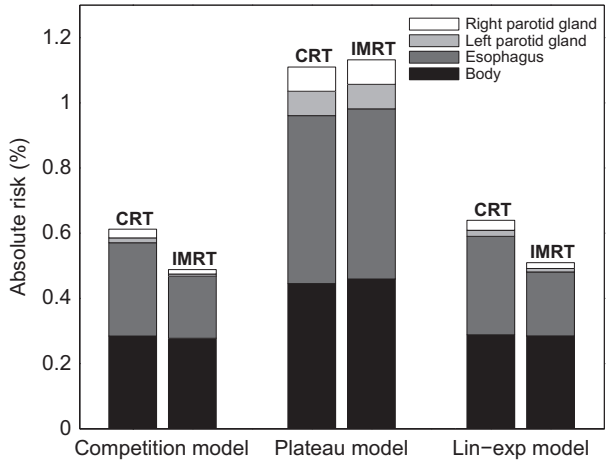

Figure 2. Average lifetime risk of developing secondary cancers from the dose burden of the primary radiation beam from IMRT and CRT. Each segment in the bars corresponds to the average calculated risk for all patients in the respective tissue.

Discussion

Several theoretical studies have investigated the impact of IMRT and other modern radiation treatment techniques on the risk for secondary cancers in long-term survivors taking into account many of the factors that could influence it [1,8–12,22–24]. Some of these studies focused on the shift from higher to lower dose levels in the normal tissues surrounding the target. When taking only this change into account, significant differences in the risks from the two treatment techniques are indeed expected irrespective of the model used. However, due to the complex anatomy in the H&N region, the shift from low to intermediate dose levels was found to be equally important, as shown by our analysis, and tends to cancel out the

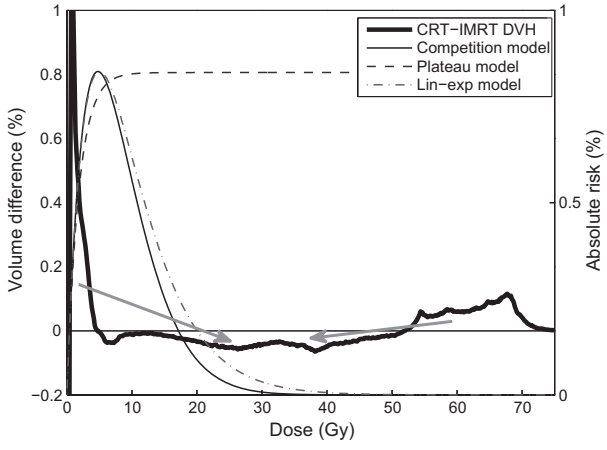

Figure 3. DVH difference for the body between IMRT and CRT for a typical H&N patient. As indicated by the arrows, IMRT shifts the dose from volumes receiving both high and low dose levels to intermediate dose levels where the plateau model predicts higher risks.

Table II. Average lifetime risk contributions from IMRT and CRT treatments (RT), scatter to the lungs, and cone-beam CT imaging.

	Competition model		Plateau model		Lin-exp model	
Risk	IMRT	CRT	IMRT	CRT	IMRT	CRT
RT without imaging	0.49%	0.61%	1.13%	1.11%	0.51%	0.64%
RT + weekly imaging	0.50%	0.62%	1.14%	1.12%	0.52%	0.65%
RT + daily imaging	0.53%	0.65%	1.17%	1.15%	0.55%	0.68%
Scatter radiation	0.58%	0.51%	0.99%	0.93%	0.58%	0.51%
Total[a]	1.08%	1.14%	2.13%	2.05%	1.10%	1.16%
Spread of total risk values	0.91–1.29%	0.91–1.48%	1.82–2.51%	1.72–2.43%	0.92–1.30%	0.93–1.50%

[a]Sum of RT with weekly imaging and scatter radiation.

former effect, leading to similar risk estimations for both techniques. This is illustrated by the results in Figure 3 showing the differential DVH of the body from a typical IMRT treatment subtracted from the corresponding differential DVH from a CRT treatment. As indicated by the arrows in the figure, IMRT implies a shift to intermediate dose levels both from high and low doses. Indeed, CRT is generally characterised by an "on-off" irradiation of the tissues around the target where the volumes in the path of the beam receive rather high doses, whilst others receive very small doses. This situation changes for IMRT where the volumes irradiated to high and low doses with CRT are redistributed to volumes receiving intermediately low doses. Thus, IMRT not only reduces high dose volumes, but also increases the intermediate dose volumes and this is an aspect that was not usually taken into account when evaluating the implications of IMRT. This trend was observed for all patients included in the present study, indicating that it might have an impact for the majority of the H&N patients receiving radiation therapy. It therefore appears that the irradiation technique used has less impact on the risk than the margins between the CTV and the PTV which were shown to have a direct impact onto the dose level in the healthy tissues surrounding the tumours [25].

The results also showed that both the plateau model and the bell-shaped models, predict similar risks for the body from IMRT and CRT. The explanation for this rather non-intuitive difference can also be found in Figure 3. Thus, the expected increase in risk for CRT in the high dose region where the plateau model predicts its maximum risk was balanced out by the contribution from the intermediate dose region where IMRT exposes a larger portion of the volume and the plateau model also predicted a large risk.

The impact of interpatient anatomical variations was investigated by comparing the predicted risks in Table II with those calculated when the volumetric factor was assumed equal to 1. Differences in the absolute risk levels were seen for some individual patients, but the relative relationships between the risks from IMRT and CRT as well as the average population risks were generally the same. Thus, the results of this study can be considered valid if interpatient variations are neglected and the volumetric factor is excluded from calculations.

Another important finding of this study was the dependence of the relative contribution of the scattered radiation with irradiation technique. Thus, when assuming the same relative contribution of the scattered radiation in all irradiation techniques, the increase in MUs associated with IMRT would also lead to an increase of the risk associated with this treatment technique. Indeed, IMRT employed on average 3.5 times more MUs than CRT. However, our results in Table I showed that CRT delivered an average increase in dose per MU with a factor of 3.3. Thus, the expected increase in dose from the more MUs employed in IMRT was cancelled out leading to similar dose contributions from scattered radiation for both treatment techniques. The difference in dose per MU between IMRT and CRT implies that assuming a single linear relationship between the absorbed dose to the patient (and implicitly the risk of developing secondary cancer for low doses) and the number of MUs required by the treatment could lead to erroneous results and should be avoided.

Furthermore, the results in Table I showed that the dose contribution from IMRT was lower compared to CRT close to the PTV and increased with increasing distance from the PTV. This could be explained by a larger influence of internal patient scatter close to the PTV which is more field-size dependent and hence favouring the smaller fields used in sliding window IMRT. Nevertheless, when excluding the doses from the first plane (inside the PTV) in the risk calculations, the risks were still comparable (0.72–0.78% for IMRT vs. 0.64–0.69% for CRT). The results indicate that the burden to the lungs from scattered radiation does not significantly increase for IMRT treatments of H&N patients. Similar findings have been reported in other studies employing more sophisticated measurements. Thus,

Vanhavere et al. [26] found that the dose contribution for 6 MV photons close to the primary field was lower for IMRT and increased only at larger distances. Also, Josteen et al. [27] reported that for breast cancer treatment the dose contribution to regions outside the primary beam was lower for IMRT in comparison to CRT.

The verification of tumour position and anatomy during treatment is essential for radiation therapy patients and requires additional irradiation that increases the radiation burden. The findings of this study showed that the dose from CBCT imaging leads only to a small relative increase of the risk that is anyhow quite low. Extrapolating these findings should however be pursued with caution, as imaging doses vary considerably depending on the equipment used [15,28] and therefore individual assessments have to be performed in each situation.

One of the important findings of this study was that there is no significant difference in risk between CRT and IMRT for radiation therapy treatment in the H&N region using 6 MV photons. The prediction of total risk for secondary cancer from modern radiotherapy techniques found in this study was between 0.9% and 2.5% depending on the risk model used. It is, however, important to acknowledge the rather large uncertainties associated with the risk models and parameters used in this study which might affect the absolute risk values listed above. Also, not all relevant tissues included in the CT data were individually delineated and used for risk estimations (e.g. the thyroid was excluded due to the uncertainties associated with its proper delineation for the patient group included in the study). Furthermore, a large part of the body (and for some patients a small portion of the oesophagus) receiving low doses was not included in the available CT data set and therefore a potential overestimation of risk in these tissues originating from Equation 1 cannot be excluded. However, these uncertainties have to be considered in the light of the primary aim of the study which was to compare the relative differences between IMRT and CRT. In this respect, the impact of model parameters uncertainties and the inclusion of further individual structures is decreased, and the important conclusion is that the risks were comparable between the two treatment techniques investigated.

The findings of the present study are comparable with the carcinogenesis risk levels from radiotherapy identified in epidemiological studies of various tumour sites [4–7] and to other theoretical risk estimations. Thus, Steneker et al. [29] estimated a 10-year risk of 1.0% for secondary tumour incidence after an H&N treatment using IMRT with 15 MV photons calculated with a lin-exp model. Similarly, using one bell-shaped and one plateau-shaped model, Ruben et al. [22] reported a carcinogenic risk of 1–2% after IMRT and CRT treatments for H&N using 6 MV photons. The slight increase in predictions in the present study could be accounted for by the use of lifetime risk estimates and by taking into account all the contributors to radiation burden relevant for this form of radiotherapy. This stresses the importance of accounting for as many dose contributors as possible when estimating the risk from radiotherapy. Indeed, data in Table II showed that scatter radiation could lead to an additional risk comparable to that from the primary radiation, in agreement with findings of epidemiological studies [6]. Also, for particle therapy or for radiation therapy with photons with higher energies than used in this study, one would have to account for the production of neutrons and other secondaries [9,23,24,28].

In conclusion, this study showed that IMRT leads to a redistribution of dose in tissue volumes from both low and high dose levels to intermediate dose levels. This redistribution of the doses to the OARs around the target with IMRT versus CRT has little impact on the overall risk. Furthermore, the risk to the lungs from scattered radiation was significant and similar for both treatment techniques. Repeated CBCT diagnostic imaging contributed little to the total risk in comparison to the treatment-associated radiation burden. Thus, the total lifetime risk from treatment, scatter radiation, and CBCT imaging was in the order of 0.9–2.5% for both IMRT and CRT. These relatively low levels of absolute lifetime risks support the use of IMRT radiation therapy with low energy photons as a viable treatment modality for inoperable or advanced H&N tumours.

Acknowledgements

The authors would like to thank Ronny Cronström for valuable help in the treatment planning process. Financial support from the County Council of Östergötland (Sweden) is also gratefully acknowledged.

Declaration of interest: The authors report no conflicts of interest. The authors alone are responsible for the content and writing of the paper.

References

[1] Hall EJ, Wuu CS. Radiation-induced second cancers: The impact of 3D-CRT and IMRT. Int J Radiat Oncol Biol Phys 2003;56:83–8.

[2] Dasu A, Toma-Dasu I, Olofsson J, Karlsson M. The use of risk estimation models for the induction of secondary cancers following radiotherapy. Acta Oncol 2005;44:339–47.

[3] Hall EJ. Intensity-modulated radiation therapy, protons, and the risk of second cancers. Int J Radiat Oncol Biol Phys 2006;65:1–7.
[4] Boice Jr. JD, Harvey EB, Blettner M, Stovall M, Flannery JT. Cancer in the contralateral breast after radiotherapy for breast cancer. N Engl J Med 1992;326:781–5.
[5] Bhatia S, Robison LL, Oberlin O, Greenberg M, Bunin G, Fossati-Bellani F et al. Breast cancer and other second neoplasms after childhood Hodgkin's disease. N Engl J Med 1996;334:745–51.
[6] Brenner DJ, Curtis RE, Hall EJ, Ron E. Second malignancies in prostate carcinoma patients after radiotherapy compared with surgery. Cancer 2000;88:398–406.
[7] Grantzau T, Mellemkjær L, Overgaard J. Second primary cancers after adjuvant radiotherapy in early breast cancer patients: A national population based study under the Danish Breast Cancer Cooperative Group (DBCG). Radiother Oncol 2013;106:42–9.
[8] Followill D, Geis P, Boyer A. Estimates of whole-body dose equivalent produced by beam intensity modulated conformal therapy. Int J Radiat Oncol Biol Phys 1997;38:667–72.
[9] Kry SF, Salehpour M, Followill DS, Stovall M, Kuban DA, White RA et al. The calculated risk of fatal secondary malignancies from intensity-modulated radiation therapy. Int J Radiat Oncol Biol Phys 2005;62:1195–203.
[10] Schneider U. Calculated risk of fatal secondary malignancies from intensity-modulated radiotherapy: In regard to Kry et al. (Int J Radiat Oncol Biol Phys 2005;62:1195–203). Int J Radiat Oncol Biol Phys 2006;64:1290.
[11] Ruben JD, Lancaster CM, Jones P, Smith RL. A comparison of out-of-field dose and its constituent components for intensity-modulated radiation therapy versus conformal radiation therapy: Implications for carcinogenesis. Int J Radiat Oncol Biol Phys 2011;81:1458–64.
[12] Abo-Madyan Y, Aziz MH, Aly MM, Schneider F, Sperk E, Clausen S, et al. Second cancer risk after 3D-CRT, IMRT and VMAT for breast cancer. Radiother Oncol 2014; 110:471–6.
[13] Hall EJ. Henry S. Kaplan distinguished scientist award 2003. The crooked shall be made straight; dose-response relationships for carcinogenesis. Int J Radiat Biol 2004;80:327–37.
[14] ICRP. ICRP Publication 103: The 2007 recommendations of the International Commission on Radiological Protection. Ann ICRP 2007;37:1–332.
[15] Palm A, Nilsson E, Herrnsdorf L. Absorbed dose and dose rate using the Varian OBI 1.3 and 1.4 CBCT system. J Appl Clin Med Phys 2010;11:3085.
[16] Quinn A, Holloway L, Hardcastle N, Tomé WA, Rosenfeld A, Metcalfe P. Normal tissue dose and second cancer risk due to megavoltage fan-beam CT, static tomotherapy and helical tomotherapy in breast radiotherapy. Radiother Oncol 2013; 108:266–8.
[17] Schneider U, Kaser-Hotz B. A simple dose-response relationship for modeling secondary cancer incidence after radiotherapy. Z Med Phys 2005;15:31–7.
[18] Davis RH. Production and killing of second cancer precursor cells in radiation therapy: In regard to Hall and Wuu (Int J Radiat Oncol Biol Phys 2003;56:83–8). Int J Radiat Oncol Biol Phys 2004;59:916.
[19] Schneider U. Dose-response relationship for radiation-induced cancer – decrease or plateau at high dose: In regard to Davis (Int J Radiat Oncol Biol Phys 2004;59:916). Int J Radiat Oncol Biol Phys 2005;61:312–3.
[20] Schneider U, Stipper A, Besserer J. Dose-response relationship for lung cancer induction at radiotherapy dose. Z Med Phys 2010;20:206–14.
[21] De Bruin ML, Sparidans J, van't Veer MB, Noordijk EM, Louwman MW, Zijlstra JM, et al. Breast cancer risk in female survivors of Hodgkin's lymphoma: Lower risk after small radiation volumes. J Clin Oncol 2009;27 :4239–46.
[22] Ruben JD, Davis S, Evans C, Jones P, Gagliardi F, Haynes M, et al. The effect of intensity-modulated radiotherapy on radiation-induced second malignancies. Int J Radiat Oncol Biol Phys 2008;70:1530–6.
[23] Brodin NP, Vogelius IR, Maraldo MV, Munck af Rosenschöld P, Aznar MC, Kiil-Berthelsen A, et al. Life years lost—comparing potentially fatal late complications after radiotherapy for pediatric medulloblastoma on a common scale. Cancer 2012;118:5432–40.
[24] Expósito MR, Sánchez-Nieto B, Terrón JA, Domingo C, Gómez F, Sánchez-Doblado F. Neutron contamination in radiotherapy: Estimation of second cancers based on measurements in 1377 patients. Radiother Oncol 2013;107: 234–41.
[25] Dasu A, Toma-Dasu I, Franzén L, Widmark A, Nilsson P. Secondary malignancies from prostate cancer radiation treatment: A risk analysis of the influence of target margins and fractionation patterns. Int J Radiat Oncol Biol Phys 2011;79:738–46.
[26] Vanhavere F, Huyskens D, Struelens L. Peripheral neutron and gamma doses in radiotherapy with an 18 MV linear accelerator. Radiat Prot Dosimetry 2004;110: 607–12.
[27] Josteen A, Matzinger O, Jeanneret-Sozzi W, Bochud F, Moeckli R. Evaluation of organ-specific peripheral doses after 2-dimensional, 3-dimensional and hybrid intensity modulated radiation therapy for breast cancer based on Monte Carlo and convolution/ superposition algorithms: Implications for secondary cancer risk assessment. Radiother Oncol 2013; 106:33–41.
[28] Gudowska I, Ardenfors O, Toma-Dasu I, Dasu A. Radiation burden from secondary doses to patients undergoing radiation therapy with photons and light ions and radiation doses from imaging modalities. Radiat Prot Dosimetry Epub 2013 Dec 18.
[29] Steneker M, Lomax A, Schneider U. Intensity modulated photon and proton therapy for the treatment of head and neck tumors. Radiother Oncol 2006;80:263–7.

Supplementary material available online

Supplementary Table I and Appendix available online at http://informahealthcare.com/doi/abs/10.3109/0284186X.2014.925581